A Patient-Derived Antibody Ameliorates Disease Severity in a Relapsing Remitting Murine Model of Multiple Sclerosis

Chad Smith,[1] Benjamin M. Greenberg,[1,2] Jack Reynolds,[1] Ryan Mosavi-Hecht,[1] Patricia Semedo-Kuriki,[1] Sara Benavides,[1] Wei Zhang,[1] Yipin Wu,[1] George Adams,[1] Bret M. Evers,[3] Kiel M. Telesford,[1,4,5] Pavel G. Yanev,[6] Marcel Mettlen,[7] Ann M. Stowe,[6,8] Doug Kerr,[9] and Nancy L. Monson[1,2,10]

Objective: Naturally occurring autoantibodies are commonly considered to be causative of autoimmune diseases or epiphenomena with no known biological impact. Although clinically beneficial autoantibodies have been described, there have been no naturally occurring anti-neuronal antibodies that have been found to be neuroprotective. Here, we identify a recombinant human antibody (TGM-010) derived from a patient with multiple sclerosis (MS) that binds human and mouse neurons, leading to beneficial effects.
Methods: TGM-010 was examined for its ability to be internalized by human and mouse neurons and protect neurons from death in vitro following a stress event. TGM-010 was also injected systemically into a relapsing–remitting model of experimental autoimmune encephalomyelitis (EAE) to examine its ability to impact disease score, extent of demyelination, and neuron frequency.
Results: TGM-010 demonstrates many novel characteristics including crossing the blood-brain barrier (BBB) and internalizing into neurons. TGM-010 also protects primary mouse neurons from death in vitro. In a mouse model of MS, TGM-010 ameliorates disease severity and is associated with improved neuronal survival.
Interpretation: This study identified a patient-derived neuron-binding autoantibody that crosses the BBB in mice and reduces neuron loss in a mouse model of MS. These data suggest that the human derived anti-neuronal antibody, TGM-010, may potentially be used to ameliorate neurodegeneration that underlies disability in neurodegenerative conditions.

ANN NEUROL 2026;00:1–14

It is well established that autoimmunity in humans is not always pathologic. Some immune responses to self-antigens can be associated with therapeutically beneficial outcomes for individuals.[1,2] The ability to identify and develop naturally occurring human autoantibodies with medicinal potential represents a novel approach to drug development. To date, no naturally occurring neuroprotective antibodies have been identified in humans and most known anti-neuronal antibodies are considered disease causing (eg, anti-NMDAR antibodies).

Patients with multiple sclerosis (MS) represent a unique patient population for many reasons. Whereas the condition was historically defined as a T-cell mediated disease,[3] we and others have demonstrated that B cells in

View this article online at wileyonlinelibrary.com. DOI: 10.1002/ana.78149

Received Jul 18, 2025, and in revised form Dec 22, 2025. Accepted for publication Dec 22, 2025.

Address correspondence to Dr Monson, Department of Neurology, The University of Texas Southwestern Medical Center, 5323 Harry Hines Blvd., Dallas, TX 75390, USA. E-mail: nancy.monson@utsouthwestern.edu

From the [1]Department of Neurology, The University of Texas Southwestern Medical Center, Dallas, Texas, USA; [2]O'Donnell Brain Institute, The University of Texas Southwestern Medical Center, Dallas, Texas, USA; [3]Department of Pathology, The University of Texas Southwestern Medical Center, Dallas, Texas, USA; [4]Department of Ophthalmology and Visual Sciences, Vanderbilt University, Nashville, Texas, USA; [5]Department of Neurology, Vanderbilt University, Nashville, Texas, USA; [6]Department of Neurology, The University of Kentucky, Lexington, Texas, USA; [7]Department of Cell Biology, The University of Texas Southwestern Medical Center, Dallas, Texas, USA; [8]Department of Neuroscience, The University of Kentucky, Lexington, Texas, USA; [9]GenrAb, Inc., Dallas, Texas, USA; and [10]Department of Immunology, The University of Texas Southwestern Medical Center, Dallas, Texas, USA

Additional supporting information can be found in the online version of this article.

patients with MS are hyper-proliferative, readily produce pro-inflammatory cytokines, and can drive Th17 responses to myelin antigens.[4,5] Yet, despite the significant activation of B cells and exposure to central nervous system (CNS) antigens, it is exceptionally rare to identify patients with MS with evidence of autoimmune encephalitis. Thus, identifying anti-neuronal B cells in patients with MS represents a unique opportunity to screen for naturally occurring neuroprotective autoantibodies.

Our laboratory cloned an antibody called TGM-010, from a patient with MS, that binds to neuronal nuclei. We previously identified enrichment of replacement mutations within antibody heavy chain family 4 (VH4) rearrangements expressed by B cells in the cerebrospinal fluid of patients who either have MS or will be diagnosed with MS in the future.[6,7] We cloned 32 of these and found that 30 of them bound to brain gray matter tissue of both mouse and human origin.[8] TGM-010 was one of these, and exhibited the most intense staining pattern to neurons in both human and mouse brain tissue.[8] Thus, we sought to determine the impact of TGM-010 on neuron health and disease trajectory in a mouse model of MS. Dogmatically, it is assumed that antibodies would not readily cross the blood-brain barrier (BBB) or internalize into neurons to bind to an intracellular antigen. Here, we show in vitro and in vivo evidence that TGM-010 is internalized by mouse cortical neurons and reduces the frequency of stress-induced death. When injected systemically into mice that have experienced a first disease attack of experimental autoimmune encephalomyelitis (EAE), TGM-010 reduces disease severity of the subsequent relapse and reduces neurodegenerative features associated with disease progression. Additionally, we show that TGM-010 crosses an intact BBB supporting the potential of using TGM-010 as a biologic agent to prevent neuronal death in patients with MS and other neurodegenerative disorders.

Materials and Methods

Recombinant Human Antibody Cloning, Expression, and Purification

The antibody variable domains of the heavy chains and light chains of the recombinant human antibodies (rhAbs) were synthesized (Integrated DNA Technologies) and cloned into IgG1 or IgK backbones provided by Dr. Michel Nussenzweig at Rockefeller University, as previously described.[9] TGM-010 (originally called AJL10) was expressed by a CD19+ B cell isolated from the cerebrospinal fluid (CSF) of a 40-year-old female patient with presentation of optic neuritis and gadolinium enhancing lesions of the brain who was subsequently diagnosed with relapsing remitting MS and has remained clinically stable for 10 years post-sampling. This study subject signed the written informed consent approved by the Institutional Review Board of the UT Southwestern Medical Center (UTSW), in accordance with the Federal-wide Assurance on file with the Department of Health and Human Services (USA). TGM-010 expresses a variable heavy chain family 4 gene (VH4-4) paired with the Joint Heavy 6 (JH6) gene and a CDR3 length of 16 amino acids with a charge of −1.005. There are a total of 16 mutations resulting in codon replacements in the heavy chain rearrangement. TGM-010 expresses a variable kappa chain family 2 gene (VK2-28) paired with the Joint Kappa 5 (JK5) gene and a CDR3 length of 9. The control rhAb for the in vitro assays was originally expressed by a blood-derived plasmablast B cell from a 28-year-old female patient with presentation of transverse myelitis and gadolinium enhancing lesions of the brain who was subsequently diagnosed with MS expressing a VH4-30:JH4 antibody heavy chain gene, a CDR3 length of 17, CDR3 charge of 0, and 13 mutations resulting in codon replacements in the heavy chain rearrangement with pairing to VK2-30:JK2 antibody kappa chain. The isotype control antibody used for the in vivo experiments was purchased from ProMab (Richmond, CA) and did not exhibit binding to brain tissue. The FreeStyle CHO-S cells (Invitrogen) were maintained in FreeStyle CHO expression media (Life Technologies). The plasmids encoding the rhAbs were transiently transfected into CHO-S cells with FreeStyle Max reagent (Invitrogen). Supernatants from these cultures were collected on day 6. The cell pellets were spun down and supernatants were passed through 0.2-μm filters and subjected to rhAb purification on the NGC Quest 10 system (BioRad). The concentrations of the rhAbs were determined by sandwich enzyme-linked immunosorbent assay (ELISA), as previously reported.[4]

Human Induced Pluripotent Stem Cell-Derived Motor Neuron Cultures

Human-induced pluripotent stem cell (iPSC)-derived motor neuron cells were purchased from Axol Bioscience (Easter Bush, UK). The cells were thawed and seeded on vitronectin- + PDL-coated coverslips (100k cells per well in a 24-well plate), maintained in motor neuron maintenance medium for plating for 24 hours, and then replaced with complete motor neuron maintenance medium, as recommended by the manufacturer. Every other day, we performed medium exchanges: full exchange for the first 2 exchanges, and then half medium changes. Cells were used for experiments on day-in-vitro 10 (DIV10).

Mouse Corticohippocampal Neuron Cultures

Prior to preparing neuron cultures, coverslips and 100-mm dishes were coated with 0.1 mg/ml Poly-L-Lysine (Sigma P2636) and incubated overnight at 37°C. The mouse corticohippocampal neurons (MCNs) were obtained from newborn (p0-p1) SJL/J mouse pups (Jackson 000686). Within a sterile biosafety cabinet under the assistance of a stereological microscope (Leica), the pups were decapitated and the cortices and hippocampi were extracted. Tissue was transferred to 2 ml dissection media (1x HBSS, Gibco 14185052; 1x Pen-Strep, Gibco 15140122; 1x pyruvate, Gibco 11360070; 10 mM

HEPES, Gibco 15630080; 30 mM Glucose, ThermoFisher A2494001). Tissue was then digested at 37°C for 15 minutes with 20 µl of 1% (w/v) DNase (Sigma DN-25) and 67 µl 20 mg/ml Papain (Worthington LS003119). The supernatant was removed, and the cells were washed twice with plating medium (Neurobasal Medium, ThermoFisher 21103049; 1x B-27, ThermoFisher 17504044; 1x Pen-Strep; 1x GlutaMax, ThermoFisher 35050061; 5% Horse Serum, GE Healthcare SH30074.03). The cell pellet was then dissociated by repeated pipetting with 3 sets of successively smaller fire-polished Pasteur pipettes, with the supernatant collected between each set. The cell suspension was run through a 70 µm cell strainer (Fisher 22363548), and then was centrifuged at 100 g × 5 minutes. The pellet was resuspended with 10 ml plating medium and counted with Trypan Blue. To produce MCNs, the cells were plated at 200,000 cells/well in 24- well plates with a final volume of 0.6 ml using plating medium. To produce companion glia cultures for use later as a media supplement source, the cells were plated at the same density as MCNs but cultured in DMEM +10% fetal bovine serum (FBS) + 1x Pen-Strep for 3 days, and then replaced with feeding medium (plating medium without horse serum) until used for MCN cultures. For MCNs, the plating medium was replaced with feeding medium after the initial 3 hours of plating. At DIV3, half the medium in the MCN cultures was replaced with fresh feeding medium supplemented with 0.5 µM Ara-C (Sigma C6645) to reduce glia outgrowth. At DIV5, the medium from 5-day glial cultures was supplemented with Ara-C and used to replenish half the medium in the MCN cultures. MCNs were used for experiments 7 days after the prep (DIV8).

Immunocytochemistry to Evaluate Neuron Binding

Cells were fixed with ice-cold 4% PFA for 10 minutes, and then washed with phosphate-buffered saline (PBS) for 5 minutes. Cells were washed with 0.2% Triton X-100 + 2 mg/ml bovine serum albumin (BSA; Sigma A9647) for 10 minutes, and then blocked with PBS + 1% goat serum (ThermoFisher 50062Z) + 3% BSA for 2 hours. Cells were incubated overnight at 4°C with primary antibodies diluted in blocking buffer: rhAbs (20 µg/ml), rabbit anti-GFAP (Abcam ab16997, 1:200), and mouse anti-MAP2 (ThermoFisher 13–1500, 1:200). The concentration of rhAbs used in this method was based on physiological measurements of single antibody clones in patients.[10–12] The next day, the cells were washed 4 × 3 minutes with 0.05% Triton X-100 + 1% goat serum +1% BSA, and then incubated for 1 hour at room temperature (RT) with secondary antibodies diluted in blocking buffer: goat anti-human conj AlexaFluor 488 (ThermoFisher A-11013, 1:1000), goat anti-rabbit conj AlexaFluor 568 (Abcam ab175471, 1:1000), and goat anti-mouse conj AlexaFluor 647 (Abcam ab150115, 1:500). The washes were repeated, and then the cells were counterstained with DAPI and washed twice with PBS. Coverslips were mounted on glass slides with Fluoromount G, then visualized on a Zeiss LSM780 confocal microscope with a 20×/0.8NA air objective lens.

Mouse Brain and Spinal Cord Tissue Preparation and Immunofluorescence to Evaluate Region Specificity

Mice were deeply anesthetized with avertin, then were perfused transcardially with PBS and 4% PFA. Their brains and spinal cords were then extracted, drop-fixed in 4% PFA for 48 hours, washed with PBS, and embedded in paraffin. Sagittal brain slices and transverse spinal cord slices (5 µm) were processed by the UT Southwestern Histo Pathology Core. Tissue slices were deparaffinized with 2 × 10-minute washes with xylenes (Fisher), and then washed with successive ethanol solutions: 2 × 100% ethanol, 95% ethanol, 70% ethanol, 50% ethanol, 30% ethanol. Slices were washed with PBS for 3 minutes, and then 1% (w/v) glycine (Sigma) for 15 minutes. Slices underwent antigen retrieval by submersion in boiling citrate retrieval buffer (Vector BioLabs H-3300) in a pressure cooker for 10 minutes, and then were allowed to cool to RT for 30 minutes. Slides were washed 2 × 5 minutes with PBS, and then with 0.2% Triton X-100 (Sigma) in PBS for 10 minutes. Slides were blocked for 2 hours with 5% goat serum + 0.1% Triton X-100 in a humidified chamber, and then incubated overnight at 4°C in a humidified chamber with primary antibodies diluted in blocking buffer: rhAbs (20 µg/ml), rabbit anti-GFAP (1:200), mouse anti-MAP2 (1:200), rabbit anti-S100b (Abcam ab52642, 1:200), and mouse anti-NeuN (ThermoFisher MA5-33103, 1:200). The next day, the slides were washed 3 × 5 minutes with 0.025% Triton X-100, and then incubated for 1 hour at RT in a humidified chamber with secondary antibodies diluted in blocking buffer: goat anti-human conj AlexaFluor 488 (1:1000), goat anti-rabbit conj AlexaFluor 568 (1:1000), goat anti-rabbit conj AlexaFluor 647 (Abcam 150,083, 1:500), goat anti-mouse conj AlexaFluor 568 (Abcam ab175473, 1:1000), and then goat anti-mouse conj AlexaFluor 647 (1:500). The rinses were repeated, and then the slides were counterstained with DAPI. The slides were washed twice with PBS and coverslips were mounted with Fluoromount G. The slides were visualized on a Zeiss LSM980 confocal microscope with a 40×/1.45 NA oil immersion lens.

Internalization and Cytotoxic Stress Assays

MCNs were used for internalization and cytotoxic stress assays on DIV8. The iPSC-derived neurons were used for internalization assays on DIV10. For internalization assays, rhAbs were diluted to 100 µg/ml in cell culture-conditioned medium, and then were added at a final concentration of 20 µg/ml to incubate at 37°C for the specified time points. The concentration of rhAbs used in this method was based on physiological measurements of single antibody clones in patients.[10–12] For 0 minutes of incubation at 37°C, the cells were refrigerated at 4°C for 10 minutes, and then incubated with rhAbs on ice for 10 minutes. Cells were washed 4 times with cold PBS prior to immunocytochemistry. Anti-tubulin (Sigma T5168, 1:1000) was used as a primary antibody, and goat anti-human superclonal conj AlexaFluor 488+ (ThermoFisher A56021, 1:1000) and goat anti-mouse conj AlexaFluor 647 (1:1000) were used as secondary antibodies. For cytotoxicity assays, rhAbs were diluted as mentioned above, added to cultures at a final concentration of

20 μg/ml, and then incubated at 37°C for 90 minutes. Then, the Caspase-3/7 Detection Reagent (ThermoFisher C10423) was added to cells at 6 μM for an additional 30 minutes at 37°C (totaling 2 hours of incubation at 37°C) prior to fixing with 4% PFA and immunocytochemistry. For neuroprotection assays, MCNs were heat-shocked at 45°C for 90 minutes to induce death. Then, the rhAbs were added at a final concentration of 20 μg/ml, along with Caspase-3/7 Detection Reagent for an additional 30 minutes (2 hours total) prior to fixing and immunocytochemistry. Cells were imaged on an LSM780 laser scanning confocal microscope. Images were analyzed with a FIJI macro. In summary, a maximum intensity projection of the image was created, then nuclei were identified through automatic thresholding of the DAPI channel. The mean fluorescence intensity (MFI) of the Caspase channel was measured within nuclei, and cells were identified as Caspase-positive through empirical thresholding of this MFI. The number of caspase-positive cells was divided by the number of total nuclei per image to calculate a percentage of dead cells. To normalize the data, all points were divided by the average of the group "Heat Shock Cells treated with control rhAb," effectively setting this group's average percentage of dead cells to 100%. To convert to viability, all datapoints were subtracted from the maximum value in the "Heat Shock Cells treated with control rhAb" group.

Blood-Brain Barrier Experiments

Wild-type SJL/J mice were injected with 125 μg control antibody or TGM-010 by intravenous (i.v.) delivery as previously established in the literature,[13] then were euthanized at either 8 or 24 hours post-injection by anesthesia with avertin and transcardial perfusion. For detection of antibodies in brain lysates, brains collected at 8 hours post-injection were homogenized using T-PER (ThermoFisher, 78510) including Protease and Phosphatase inhibitor cocktail (ThermoFisher, 78442) and a bead-based homogenizer. A 96-well plate was incubated overnight with 2 μg/ml goat anti-human IgG (Jackson Immune Research, 109-005-088). After discarding the supernatant, the plate was blocked with 3% Blocker A in PBS (MesoScale, R93AA) for 1 hour. The plate was washed 3 times with PBS + 0.1% Tween-20, and then incubated for 2 hours with standards and samples. The washes were repeated, then the plate was incubated with 1 μg/ml Sulfo-Tag Labeled anti-Human Antibody (MesoScale, R32AC). The washes were repeated, then the wells were incubated with GOLD Read Buffer B (MesoScale, R60AM) and read on a MESO QuickPlex 120 SQ 120MM. For the imaging studies, the mice were perfused and the brains collected at 8 and 24 hours post-injection were harvested, and then fixed as described above, and cryopreserved in PBS + 30% (w/v) sucrose (Fluka 84097). Brains for the imaging studies were frozen in OCT, then 30 μm sections were obtained with a sliding microtome (Leica) and stored in cryoprotectant buffer (30% glycerol + 30% ethylene glycol in PBS) at −20°C. Sections were washed in PBS for 10 minutes, and then incubated in a blocking buffer consisting of 0.1% Triton X-100 + 1% goat serum + 1% BSA in PBS for 1 hour. Sections were then incubated with primary antibodies in blocking buffer overnight at 4°C: Mouse anti-NeuN (1:1000, EMD Millipore MAB377). The next day, the sections were rinsed 3 × 10 minutes in 0.1% Triton X-100, then incubated with secondary antibodies for 1 hour in blocking buffer: goat anti-human conj AlexaFluor 488 (1:1000) + goat anti-mouse conj AlexaFluor 568 (1:500) + DAPI. The rinses were repeated, then the brain sections were mounted on slides. Slides were visualized on a Zeiss LSM980 confocal microscope with a 40×/1.45NA oil immersion lens. Neurons were identified by expression of NeuN and fluorescence intensity of the rhAb channel was quantified with FIJI.[14] Neurons were identified as rhAb-positive through iLastik, and images were registered to the Allen Brain Atlas. Animations were generated using Imaris (Oxford Instruments).

Experimental Autoimmune Encephalomyelitis and Therapeutic Administration of Antibodies

Female SJL/J mice (Jackson 000686) were induced for EAE at 7 to 8 weeks of age. Mice were briefly anesthetized with isoflurane, then injected s.q. with 25 μg $PLP_{139\text{-}151}$ + 50 μg CFA in PBS adjacent to the axillary and lumbar lymph nodes. Mice were observed for recovery, then EAE scores were recorded at least daily until the termination of the experiments as follows by personnel blinded to treatment.

The EAE scoring scale is as follows: 0.0 = no discernable symptoms; 0.5 = tip of tail is limp; 1.0 = limp tail; 1.5 = limp tail and hindlimb inhibition; 2.0 = limp tail and hindlimb weakness; 2.5 = limp tail and dragging of hindlimbs; 3.0 = limp tail and complete paralysis of hindlimbs, or almost complete hindlimb paralysis, or paralysis of one front and one hindlimb; 3.5 = limp tail and hindlimb paralysis, in addition to inability to right itself or flat hindquarters; and 4.0 = limp tail, complete hindlimb and partial forelimb paralysis. Mice were euthanized in case of severe paralysis or weight loss.

Mice with EAE scores of 2.5 or greater for at least 2 consecutive days during the initial demyelinating episode (initial attack) were included in the experiment. A second criteria for inclusion was remission of the initial demyelinating episode defined as EAE score of 1.5 or below between day 17 and 19 post-EAE induction. Mice were excluded from analysis if they displayed atypical EAE symptoms, such as head-tilting or axial rotation.

For intracranial injections, mice were randomized for treatment and injected in the lateral ventricle with 5 μg of antibodies as previously established.[15] For intraperitoneal injections, mice were randomized for treatment with 200 μg of control antibodies or TGM-010 beginning on day 19 post-induction, and administered every other day for a total of 6 injections. The dosage of 200 μg was determined based on previous studies concerning antibody treatment in EAE mice.[16] At the completion of the experiment, the mice were perfused transcardially with PBS and 4% PFA. Brains and spinal cords were extracted, drop-fixed in 4% PFA for 48 hours, washed with PBS, and embedded in paraffin. Sagittal brain slices and transverse spinal cord slices (5 μm) were processed by the UT Southwestern Histo Pathology Core.

Post-EAE Demyelination and Inflammation Evaluations

Hematoxylin and eosin (H&E) plus Luxol Fast Blue (LFB) staining was performed on spinal cords by the UTSW Histo Pathology Core as follows. Slides were deparaffinized in 95% ethanol and subsequently incubated overnight at 57 to 60°C in 0.1% Luxol Fast Blue solution. After incubation, white and gray matter was differentiated by immersion in 0.05% lithium carbonate, followed by serial changes of 70% ethanol with continuous monitoring to prevent over-differentiation. Upon completion of Luxol Fast Blue staining, slides were rinsed in water and processed for routine H&E staining using a Sakura Prism Plus x-y-z robotic stainer with Leica Selectech reagents (Hematoxylin 560 and Alcoholic Eosin Y 515). Slides were then cover slipped with Permount Mounting Medium (Fisher Scientific SP15-100). The slides were then digitally scanned using an Aperio GT 450 system (Leica Biosystems). Semi-quantitative scoring of cellular infiltrate was performed by a blinded board-certified neuropathologist as follows: 0 = no inflammation; 1 = cellular infiltrate only in the perivascular areas and meninges; 2 = mild cellular infiltrate in parenchyma; 3 = moderate cellular infiltrate in parenchyma; and 4 = severe cellular infiltrate in parenchyma. Additionally, the percent area of demyelination to the total area of white matter was calculated using QuPath software.

Post-EAE Neuron Enumeration

Confocal images of the sacral spinal cord were cropped to include only the ventral region by drawing a rectangular region of interest (ROI) around the lower half of the tissue, where the lower half was defined by the midpoint of the central canal. An ImageJ macro was then used to enumerate NeuN positive cells within this region in the following basic steps: automatic thresholding (default method), binary mask conversion, binary hole filling, binary close operation, adjustable watershed processing, and particle analysis.

Statistical Analyses

Analyses were performed with GraphPad Prism 10 software. Two-way analysis of variance (ANOVA) was used to compare analyses over multiple timepoints. One-way ANOVA was used to compare most other experiments, unless there were <3 groups in which case a Student's t test was appropriate. Data are represented as mean ± SEM (ns = not significant; *: $p \leq 0.05$; **: $p \leq 0.01$; ***: $p \leq 0.001$; and ****$p \leq 0.0001$).

Results

TGM-010 Binds Human and Mouse Neuronal Nuclei

Previous experiments examining B cells from the CSF of adult patients with MS identified several antibodies that preferentially bound neuronal soma in the gray matter of human brain and mouse cortex.[8] Among these neuron-binding antibodies was TGM-010 (previously called AJL10), a VH4+ antibody that exhibited notably stronger binding to neuronal nuclei than others evaluated in these early characterization studies.[8] To verify binding to human and mouse neuronal nuclei, we used iPSC-derived human neurons and primary MCNs to examine co-localization of TGM-010 with these neuron types and verify localization to the nucleus. Indeed, TGM-010 bound to MAP2+ human iPSC-derived motor neurons (Fig 1A) and MAP2+ primary MCNs (Fig 1C), specifically in the nucleus. In contrast, the control rhAb failed to bind these cells (Fig 1B, D). These results indicate that TGM-010 binds human and mouse neuronal nuclei. We next used whole mouse brain tissue to examine the binding of TGM-010 to specific brain regions. As indicated in Supplementary Figure S1A, TGM-010 binds neurons in the gray matter of wild-type (WT) mouse cortex, but not white matter in the corpus callosum, as we had observed earlier with human brain tissue from a patient with MS S1A.[8] Closer examination of the hippocampus confirmed TGM-010 colocalized with NeuN+ neurons, but not S100b+ astrocytes (Fig 1E). Similar neuron-binding was observed in pyramidal layer of the hippocampal formation and the granule layer of the dentate gyrus (Supplementary Fig S1C and Fig 1E). Notably, the control rhAb did not exhibit binding within these regions (Supplementary Fig S1B, D and Fig 1F). Neuron-binding by TGM-010 was also detected throughout the gray matter of spinal cord tissue derived from WT mice, whereas the control rhAb did not bind to this tissue (Supplementary Fig S1E, F).

TGM-010 is Internalized by Neurons and Protects Against Neurotoxic Stress

To examine the binding pattern of TGM-010 in live cells, we harvested primary MCNs from postnatal mice and incubated them with TGM-010 (Fig 2A). We found that TGM-010 was rapidly internalized into the nuclei of MCNs within 30 minutes (Fig 2B, C–G). In contrast, a control antibody was not internalized into the nuclei of MCNs over time (Fig 2B, H–L). We confirmed these results in human iPSC-derived motor neurons, detecting internalized TGM-010 (but not the control rhAb) in the nuclei within 30 minutes (Supplementary Fig S2). These results demonstrate that TGM-010 transitions across the cell membrane of human and mouse neurons.

To determine the impact of TGM-010 on neuronal health, we adapted an in vitro method to induce neuronal death via thermal stress in MCNs.[17] We used Caspase 3/7 activity as an indicator of early non-reversible death pathway engagement[18] to focus our studies on acute impact (Fig 3A). In this context, neuron viability declines

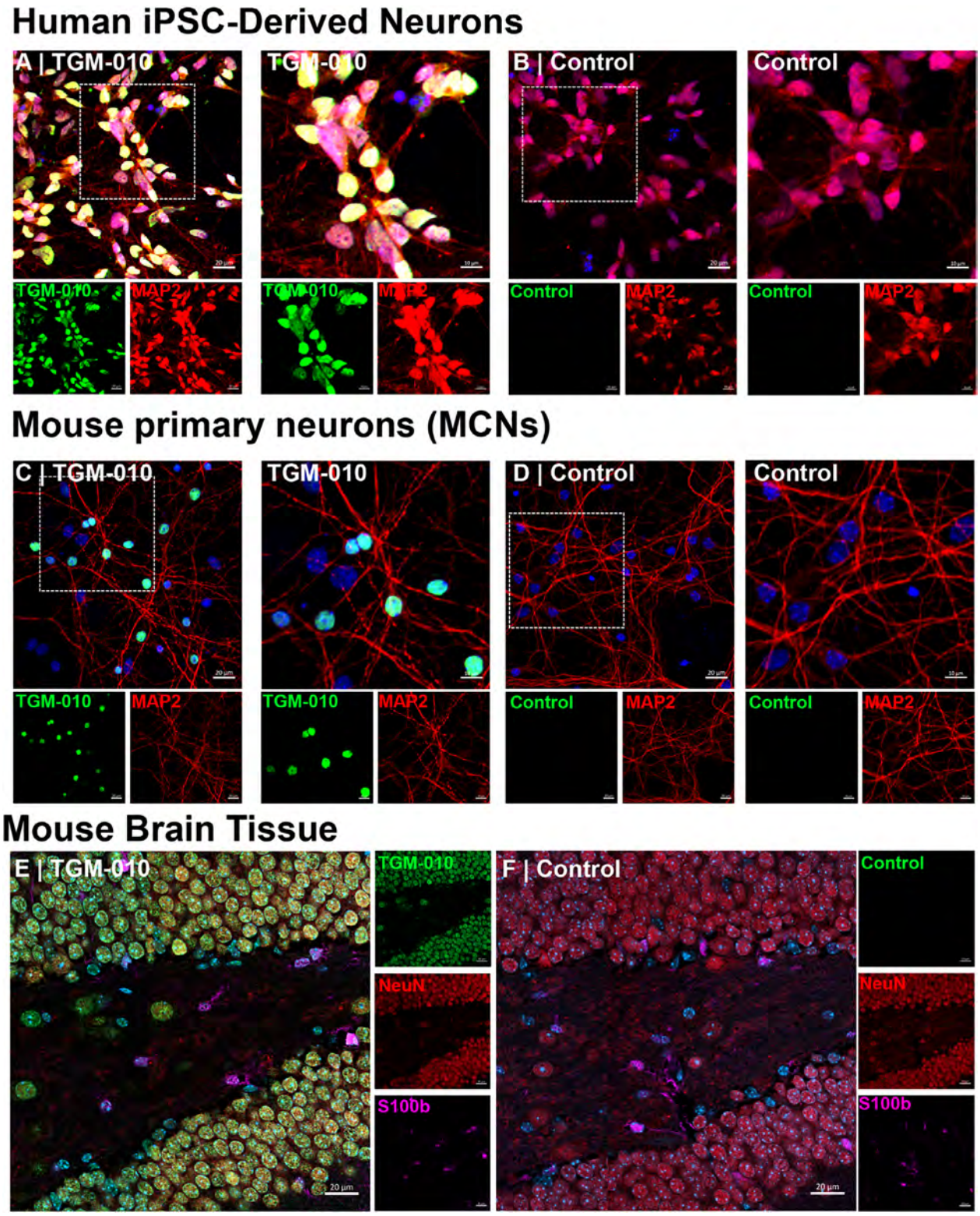

FIGURE 1: TGM-010 binds human and mouse neuronal nuclei. Representative images of iPSC-derived human motor neurons showing binding of TGM-010 (A) but not a control rhAb. (B) The insets to the right of A and B show subsets of neurons from A and B at higher magnification. Green = rhAb; red = MAP2; and blue = DAPI. Representative images of mouse primary neurons showing binding of TGM-010 (C) but not a control rhAb. (D) The insets to the right of C and D shows subsets of neurons from C and D at higher magnification. Green = rhAb; red = MAP2; and blue = DAPI. Representative images from a fixed WT mouse brain showing binding of TGM-010 (E), but not a control rhAb (F) to NeuN+ neurons in the dentate gyrus. Green = rhAb; red = NeuN; violet = S100b; and blue = DAPI. iPSC = induced pluripotent stem cell; rhAb = recombinant human antibody; WT = wild-type.

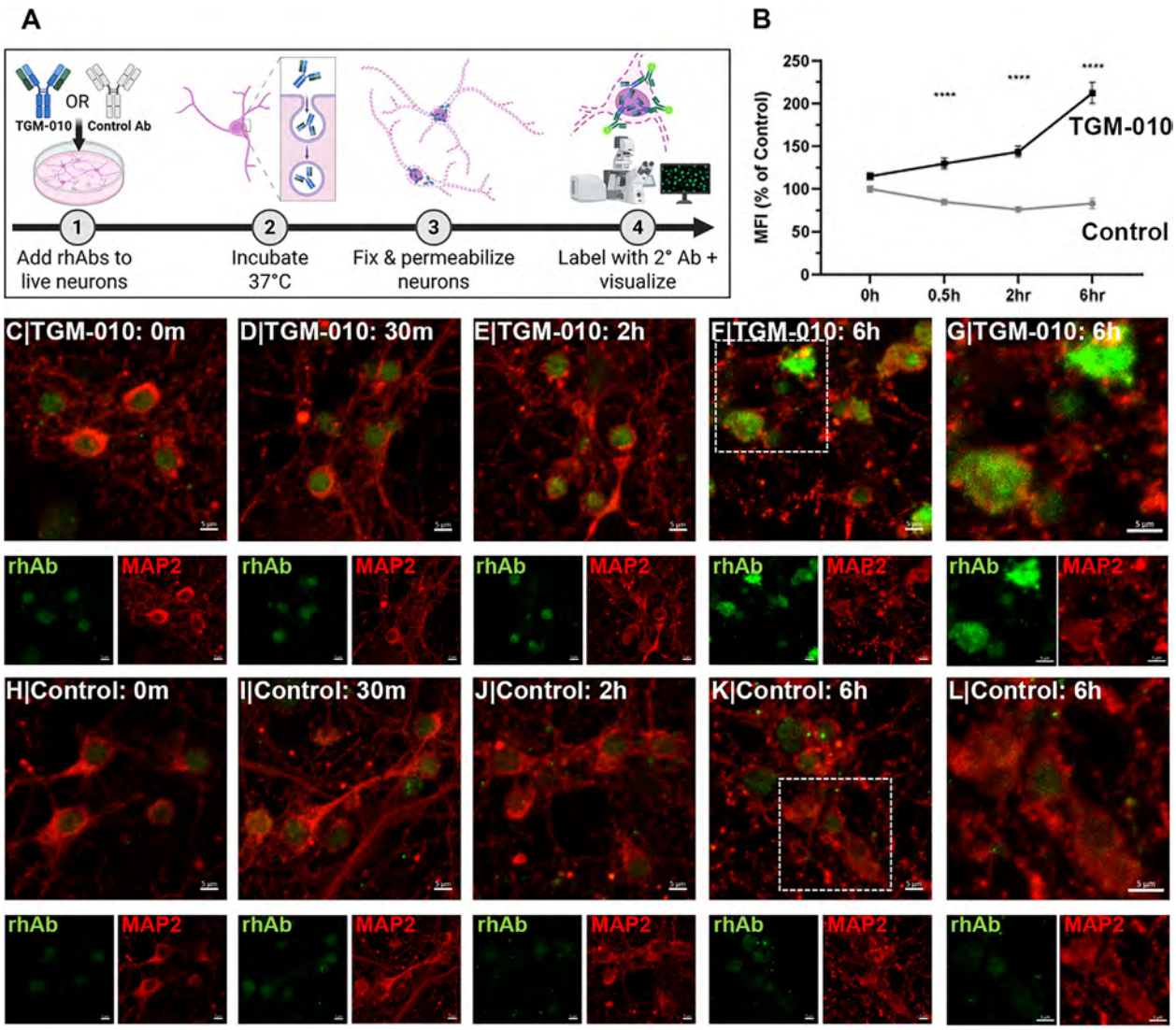

FIGURE 2: TGM-010 is internalized by primary mouse neurons in vitro. (A) Schematic of the experiment workflow. (B) Quantification of mean fluorescence intensity of TGM-010 and control antibody internalization within mouse neuronal soma. (C–G). Representative images from TGM-010 internalization to MAP2+ primary neurons. (H–L) Representative images from control antibody internalization to MAP2+ primary neurons. G and L show an inset of neurons from F and K. Green = rhAb; and red = MAP2. rhAb = recombinant human antibody.

such that only 20% of neurons remain Casp3/7negative after 2.5 hours of thermal stress (Fig 3B) and continues to decline for up to 8 hours (data not shown). In contrast, thermally stressed MCNs treated with TGM-010 maintained nearly 100% viability (Fig 3C). Thermally stressed MCNs treated with the control antibody had significantly reduced viability compared with MCNs treated with TGM-010 (see Fig 3C, E–G). MCN viability was not impacted by exposure to TGM-010 or the control rhAb in the absence of thermal stress (Fig 3D). Total neuronal density was not affected by heat shock or antibody treatment (Supplementary Fig S3A–C). This suggests that exposure to TGM-010 reduces MCN toxicity caused by thermally induced neuronal stress.

TGM-010 is Internalized by Neurons In Vivo and Modulates Relapse in a Mouse Model of MS

The in vitro data suggested that TGM-010 modulates stress-induced neuronal death. To examine this in the context of MS, we first verified that TGM-010 could be detected in the CNS of mice systemically injected with TGM-010 or the control rhAb. To do this, 125 μg of TGM-010 or the control antibody was injected into the tail vein of WT female SJL/J mice and brain tissue was harvested at 8 and 24 hours post-injection (Fig 4A). TGM-010 was detected in brain lysate at 8 hours post-injection (Fig 4B), neurons within the cortex of mouse brain tissue 8 and 24 hours post-injection (Fig 4C–E) and throughout the brain at 24 hours post-injection by tail

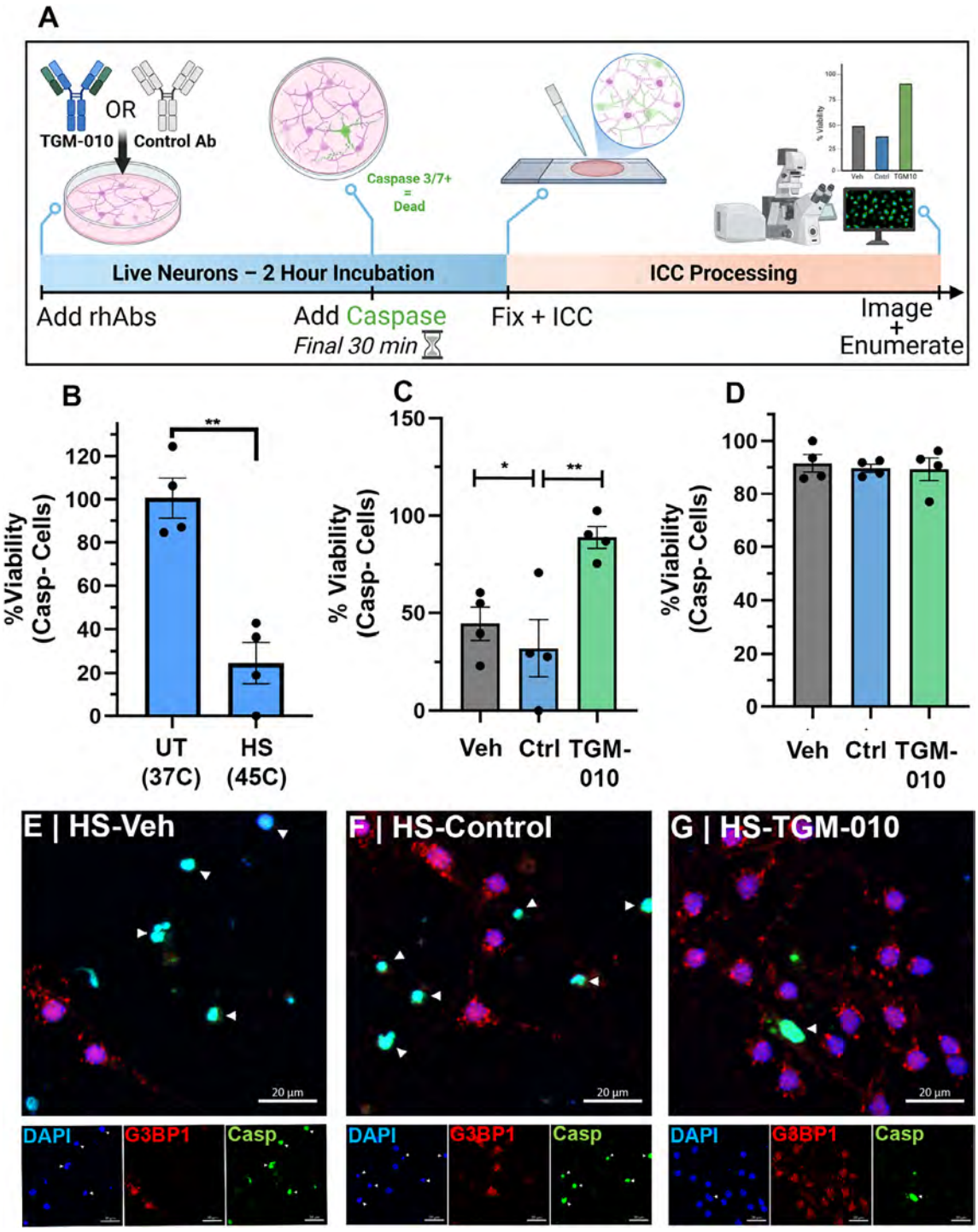

FIGURE 3: TGM-010 protects against neurotoxic stress. (A) Schematic of the experiment workflow. (B) Quantification of neuronal viability after incubation at 37°C (UT) or 2 hours thermal stress at 45°C (HS). (C) Quantification of neuronal viability after thermal stress, with incubation of vehicle, a control rhAb, or TGM-010 post-stress induction. (D) Quantification of neuronal viability after incubation at 37°C (UT) with incubation of vehicle, a control rhAb or TGM-010. (E–G) Representative images from mouse primary neurons incubated with a vehicle control (E) control rhAb (F), or TGM-010 (G) and induced for thermal stress. *N* = 4 images/group, *: $p \leq 0.05$, **: $p \leq 0.01$ by 1-way ANOVA. ANOVA = analysis of variance; HS = heat shocked; rhAb = recombinant human antibody; UT = untreated.

vein (Supplementary Video S1). There was no significant difference in the neuron density of mice treated with TGM-010 or the Control antibody at 8 or 24 hours post-injection (see Supplementary Fig S3D).

To examine the potential neuroprotective effects of TGM-010 in vivo, we used the relapsing-remitting MS model in the SJL/J strain, as female SJL/J mice typically undergo an initial demyelination episode within 10 to

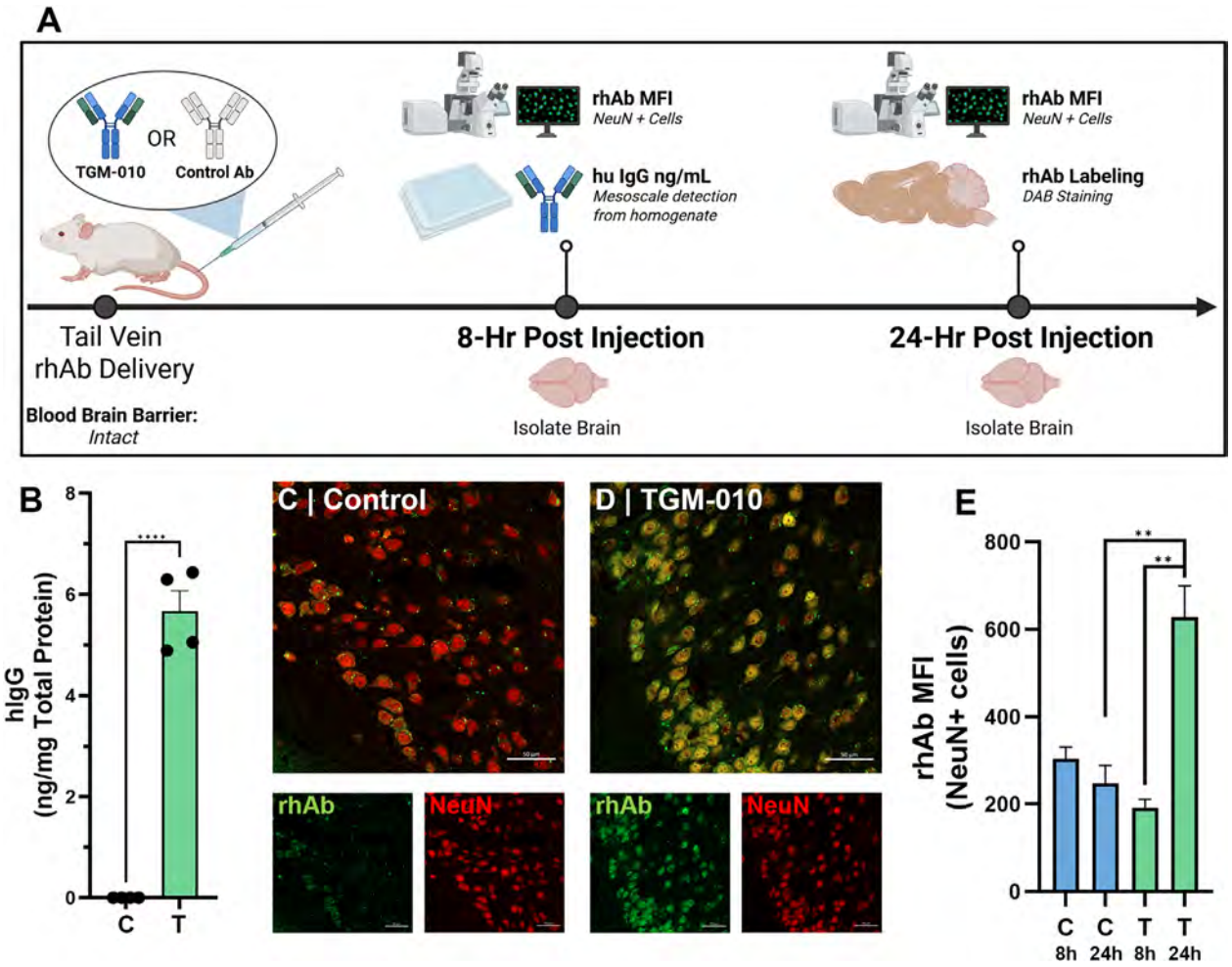

FIGURE 4: TGM-010 is internalized by neurons in vivo. (A) Schematic of the experiment workflow. (B) Quantification of rhAb in brain lysates of mice following intravenous delivery of TGM-010. **** $p \leq 0.0001$ by *t* test. (C, D) Representative images from the entorhinal cortex of a WT mouse following intravenous delivery of control rhAb (C) or TGM-010 (D) 24 hours post-injection. Green = rhAb; and red = NeuN. (E) Quantification of rhAb signal in NeuN+ cells. N ≥ 500 cells/group. ** $p \leq 0.01$ by 2-way ANOVA. ANOVA = analysis of variance; rhAb = recombinant human antibody; WT = wild-type.

12 days of induction that is characterized by tail and limb weakness, paralysis,[19] and inflammation.[20,21] This episode lasts a few days, then the mice experience a remission, followed by relapsing episodes during which time axon loss is observed.[20,21] We induced disease and selectively identified mice that experienced a severe initial episode, then treated them with TGM-010 or the control rhAb during remission in 2 delivery approaches: (1) intracerebroventricular (ICV) injections to remove the confounder of BBB integrity on the results and (2) intraperitoneal (i.p.) injection to query the potential confounder of BBB integrity on the results. In the ICV injection model, TGM-010 or the control rhAb were injected once at the remission stage, and blinded score monitoring continued until euthanasia at day 31 post-EAE induction (Supplementary Fig S4A). In this ICV model, TGM-010 reduced EAE scores compared to control (Supplementary Fig S4B) and TGM-010 could also be detected in the hippocampus (Supplementary Fig S4C, D).

In the i.p. injection model, TGM-010 or control rhAb were injected every 48 hours for 6 treatments at the remission stage, and blinded score monitoring continued until euthanasia at day 31 post-EAE induction (Fig 5A). In this i.p. model, mice treated with the control rhAb exhibited increased severity of disease disability during the relapse phase, whereas mice that were treated with TGM-010 exhibited reduced severity of disease disability (Fig 5B). Additionally, mice treated with TGM-010 displayed significantly less white matter demyelination in the lumbar-sacral region of spinal cords (Fig 5C,E,F), and reduced cellular infiltrate in the spinal cord (see Fig 5D–F) compared with control-treated mice. Loss of NeuN+ neurons provides evidence of neurodegeneration in the EAE model[22,23] particularly at this later stage of EAE.[20,21] Indeed, mice treated with TGM-010 exhibited an

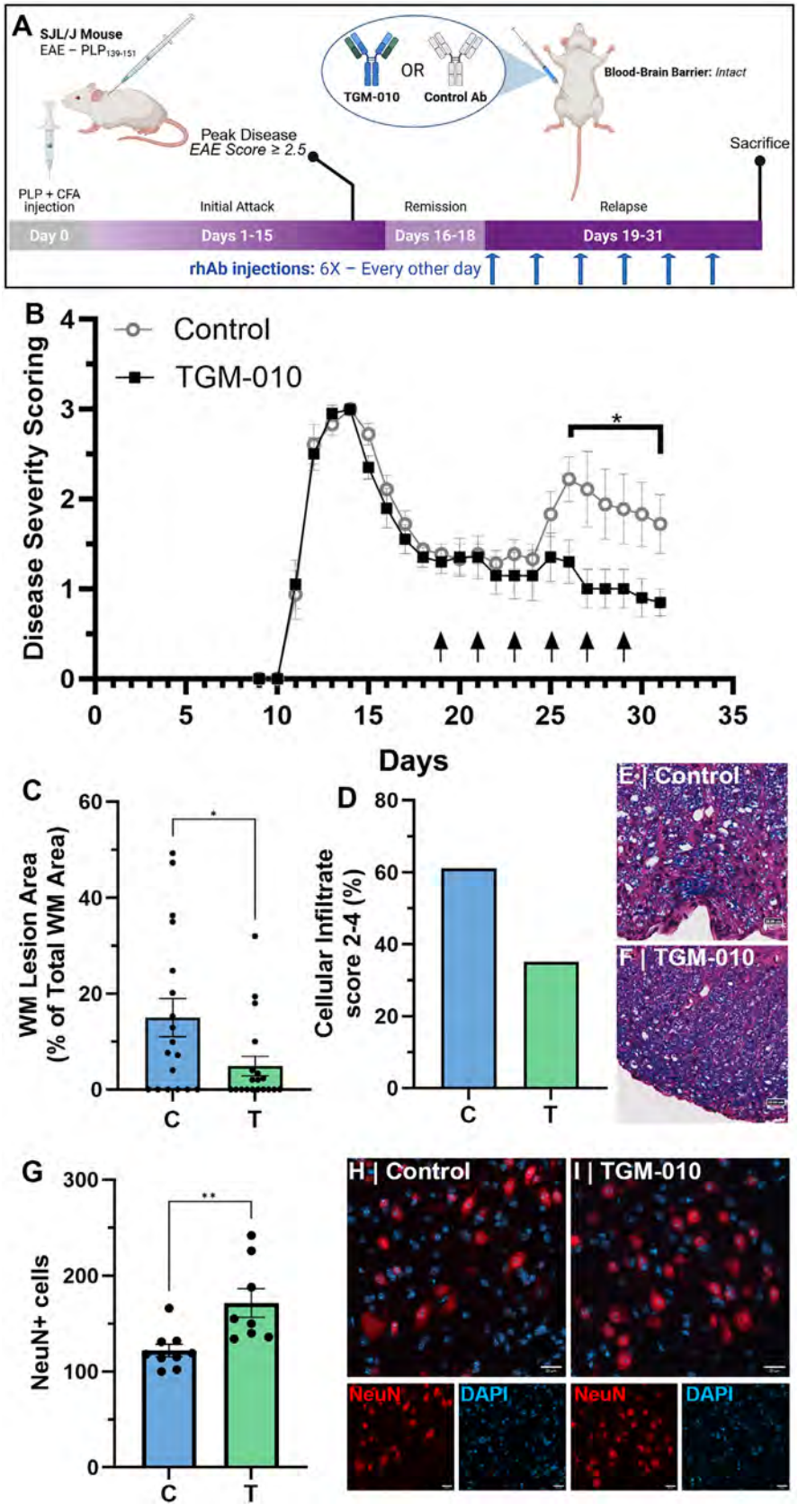

(Figure legend continues on next page.)

increased frequency of neurons compared with control-treated mice (Fig 5G–I).[24] These data demonstrate that TGM-010 reduces disease severity and neuronal loss in this model of MS. Of note, mice experienced similar symptom features of the initial attack and remission(Supplementary Fig S5A–N). Other symptom features of the relapse including day of peak severity, time from remission to peak severity, and cumulative score of the relapse phase were significantly different between the control-treated and TGM-010-treated mice (Supplementary Fig S5O–R). Animal mass was not impacted (Supplementary Fig S5S).

Discussion

Autoantibodies in the context of CNS disease have classically either been categorized as (1) epiphenomena with no impact on disease pathology or (2) pathological with a direct link to disease cadence.[25–28] Of note, these autoantibody categorizations are based largely on whether the antigen target is intracellular or expressed on the cell surface. Autoantibodies targeting intracellular antigens have been considered epiphenomena with no pathological potential. This is a widely accepted conclusion based on the presumption that autoantibodies are incapable of being internalized by intact neurons thereby limiting target interactions.[25–27] One early exception has been the anti-YO antibodies associated with paraneoplastic cerebellar degeneration (PCD) which are internalized by neurons and induce neuronal death in vitro.[29,30] Histopathological examination of cerebellar tissues of patients with PCD and high titers of anti-YO autoantibody display features of both neuroinflammation and neurodegeneration.[31] In MS, neuroinflammation and neurodegeneration are documented to drive pathology, and disability has been linked directly to loss of neurons. TGM-010 is an anti-neuronal antibody targeting an intracellular antigen that was cloned from a B cell in the cerebrospinal fluid of a patient with MS.[4,8] Here, we demonstrate that TGM-010 is internalized by live neurons. But rather than inducing cell death, this anti-neuronal antibody protects neurons from death.

The premise of TGM-010 as a therapeutically useful neuroprotective antibody in the CNS would require it to cross the BBB. By convention, antibodies cross the BBB using uncontrolled nonspecific protein brain entry or the endogenous transport system of receptor-mediated transcytosis (RMT).[32] Thus, many ongoing studies championing the use of antibodies as biologicals in the treatment of CNS disease are focused on identifying modifications of the Fc portion of antibodies that would enhance BBB transcytosis and uptake into the central nervous system.[32–35] For example, the anti-BACE1 human IgG1 antibody is designed to clear amyloid beta from brains of patients with Alzheimer's disease, but only demonstrated efficacy with the modified antibody version that had higher penetrance to the brain.[35] In the case of TGM-010, the unmodified version crosses the BBB even in WT mice that have not experienced inflammation or reduced integrity of the BBB. Elucidating the mechanism of internalization and retention of TGM-010 in the brain and, in particular, neurons, is one focus of our future investigations.

The underlying disability and disease progression in patients with MS is due to the slow degeneration of neurons as measured by reduced neuron density.[36–40] Despite a multitude of immunotherapies to treat MS, there are currently no therapies available to directly abrogate neuronal cell death[41,42] as evidenced by well-documented continuance of progression despite effective immunomodulation.[37,43–45] In the PLP-SJL EAE model,[21] disability following the initial attack is driven by the extent of neuronal loss as it is in patients with MS.[36–40] Thus, we tested the impact of TGM-010 treatment following the initial attack on disability scores and neuron density in this model. Treatment with TGM-010 following the initial attack reduces disability quantified by EAE scoring and preserves neuron density. To our knowledge, there is no other anti-neuronal antibody documented to impact EAE disease in this manner.[46] We speculate that TGM-010 ameliorates disease severity in this relapsing-remitting model of EAE by altering neuronal function in a manner that enhances resilience to the long-term impact of initiating insult(s).

FIGURE 5: TGM-010 modulates relapse in a mouse model of MS. (A) Schematic of the experimental workflow. (B) Average of daily EAE scores of a cohort of EAE mice treated with a control antibody (*grey*) or TGM-010 (*black*). Arrowheads indicate the days after induction in which mice were treated with rhAbs. N = 11–12 mice/group. *: $p \leq 0.05$ by 2-way ANOVA. (C) Area of demyelination in lumbar and sacral spinal cord of mice treated with a control rhAb or TGM-010 on day of euthanasia (d31). N = 18 to 19 sections, 9 to 10 mice per group. *: $p \leq 0.05$ by *t* test. (D) Frequency of mice at inflammatory infiltrate score of 2 to 4 within the lumbar-sacral spinal cord on day of euthanasia (d31). N = 18 to 20 sections, 9 to 10 mice per group. (E, F) Representative images of H&E/LFB staining showing demyelination and inflammatory infiltrate in mice treated with control antibody (E) or TGM-010 (F). (G) Quantification of NeuN+ neurons in spinal cords of mice treated with control rhAb or TGM-010. **: $p \leq 0.01$ by *t* test. (H, I) Representative images of NeuN+ cells in ventral lumbosacral spinal cord of mice treated with a control rhAb (H) or TGM-010 (I). Blue = DAPI; and red = NeuN. ANOVA = analysis of variance; EAE = experimental autoimmune encephalomyelitis; H&E = hematoxylin and eosin; LFB = Luxol Fast Blue; MS = multiple sclerosis; rhAb = recombinant human antibody; WM = white matter.

Alternatively, TGM-010 may correct homeostatic imbalance rather than interfere in the autoimmune response. Indeed, TGM-010's ability to protect neurons against thermal stress in vitro, in the absence of immune cells, supports these concepts. However, neurodegeneration following disease initiation is also influenced by the degree of inflammation, glutamate toxicity, mitochondrial dysfunction, and oxidative stress. Thus, our observation that, at this later stage of EAE, TGM-010 also reduces features of neuroinflammation including cellular infiltrate and extent of demyelination is not unexpected. Nevertheless, examining the impact of TGM-010 treatment on the initial demyelinating event (preventative model) when cellular infiltration and demyelination is high[20,21] would also be of interest and may further extend the efficacy of TGM-010 to early stages of disease.

Our focus here was the efficacy of TGM-010 treatment at a later stage of established disease to examine its impact on features of neurodegeneration including progression of disability measured by EAE scores and reduced neuron density. This therapeutic treatment model approach also conveyed scientific rigor by treating mice that displayed high disease severity prior to treatment. However, we identified several limitations to the study, including the lack of biomarker panels that further define features of neurodegeneration in MS and its mouse models.[47–49] For example, others have shown that the frequency of stress granule puncta is a measure of neurodegeneration in EAE,[23] but the extent of neuronal death in the control-treated mice combined with a later experimental endpoint in our approach limited our ability to quantify SG puncta. Future studies should incorporate emerging biomarkers and approaches to further define features of neurodegeneration impacted by treatment with TGM-010. A second limitation is that whereas we used well-established methods to quantify cellular infiltration and demyelination,[50–53] the composition of the cellular infiltrate (ie, microglia, and T cell and B cell frequencies)[20] and quantification of myelin basic protein (MBP)[54] was not incorporated into this dataset. Future studies should include detailed examination of the cellular infiltrate and quantification of MBP-specific demyelination to further elucidate more specifically the impact of TGM-010 on disease progression. Finally, it should be noted that whereas TGM-010 impacts several features of EAE disease, other rhAbs we had examined in the original publication also displayed neuron binding properties,[8] which we later verified was largely isolated to VH4+ rhAbs.[4] Future studies should focus on examining if these other VH4+ neuron binding rhAbs also display neuroprotective properties like TGM-010.

In conclusion, we have identified an antibody expressed by a B cell from the cerebrospinal fluid of a patient with MS with neuroprotective properties both in vitro and in vivo. To our knowledge, TGM-010 is the first human-derived antibody identified that can prevent or reduce neuronal death which underlies disease progression in MS and neurodegenerative disorders more broadly. Within patients with MS, other neurodegenerative disorders, and the EAE model, clinical disability is correlated with neuronal loss. In the context of inflammatory stress, neurons are triggered to undergo apoptosis thereby causing long lasting clinical disability. TGM-010 enters the brain and specifically enters neurons. In the setting of chronic inflammation, neurons are protected from death and EAE mice have lower disability scores. The next steps would be to identify the antigen target and investigate how (1) TGM-010 modulates this pathway to impact disease progression and (2) whether other patients with MS exhibit antibody binding to this target antigen. Understanding whether the neuroprotective properties of TGM-010 are unique, shared among other rhAbs or prevalent in other patients, is of great importance but was not addressed here. Because many of the other CNS-centric diseases are hallmarked by ongoing neurodegeneration, such studies into the mechanism by which TGM-010 modulates neurodegeneration may inform toward a broader use.

Acknowledgment

The authors thank our patients and their families for continuing to support our program efforts by donating samples for research. We cannot do this without you. We thank Chaitanya Joshi and Matthew Hein for their diligence in performing antibody delivery in some of the EAE experiments. We thank Erik Plautz in the Whole Brain Microscopy Facility (Director, Dr Denise Ramirez) for assisting intrathecal and intracerebroventricular delivery of antibody in the EAE experiments. Experimental overview panels in the figures were generated using BioRender. This project was funded by a sponsored research agreement with GenrAb and Research Bridge Partners to Dr Monson. The Whole Brain Microscopy Facility was funded by award SCR_017949, the Quantitative Light Microscopy Core was funded by award 1P30CA142543-01 and the Zeiss Axioscanner 7 was funded by award 1S10OD032267-01.

Author Contributions

Chad Smith: Conceptualization; investigation; writing – original draft; methodology; validation; visualization; writing – review and editing; software; formal analysis; project administration; data curation; supervision.

Benjamin M. Greenberg: Conceptualization; funding acquisition; writing – original draft; writing – review and editing. **Jack Reynolds:** Validation; investigation; writing – review and editing. **Ryan Mosavi-Hecht:** Investigation; validation; visualization; methodology; writing – review and editing; formal analysis. **Patricia Semedo-Kuriki:** Formal analysis; writing – review and editing; visualization; methodology. **Sara Benavides:** Visualization; writing – review and editing; formal analysis; resources. **Wei Zhang:** Investigation; methodology; writing – review and editing; writing – original draft; resources. **Yipin Wu:** Investigation; writing – original draft; writing – review and editing; methodology. **George Adams:** Methodology; writing – review and editing; resources. **Bret M. Evers:** Methodology; writing – review and editing. **Kiel M. Telesford:** Conceptualization; methodology; writing – review and editing. **Pavel G. Yanev:** Methodology. **Marcel Mettlen:** Conceptualization; methodology; writing – review and editing; visualization. **Ann M. Stowe:** Methodology; conceptualization; writing – review and editing; visualization. **Doug Kerr:** Conceptualization; writing – review and editing. **Nancy L. Monson:** Conceptualization; investigation; funding acquisition; writing – original draft; methodology; validation; visualization; writing – review and editing; data curation; supervision; resources.

Potential Conflicts of Interest

The authors have nothing to report.

Data availability

Data are available upon request to the corresponding author. Supplementary material is available online in the journal.

References

1. Greenberg BM, Bowen JD, Alvarez E, et al. A double-blind, placebo-controlled, single-ascending-dose intravenous infusion study of rHIgM22 in subjects with multiple sclerosis immediately following a relapse. Mult Scler J 2022;8:20552173221091475.
2. Mattos MS, Vandendriessche S, Schuermans S, et al. Natural antibodies are required for clearance of necrotic cells and recovery from acute liver injury. JHEP Rep 2024;6:101013.
3. Weiner HL. Multiple sclerosis is an inflammatory T-cell-mediated autoimmune disease. Arch Neurol 2004;61:1613–1615.
4. Rivas JR, Ireland SJ, Chkheidze R, et al. Peripheral VH4+ plasmablasts demonstrate autoreactive B cell expansion toward brain antigens in early multiple sclerosis patients. Acta Neuropathol 2017;133:43–60.
5. Ireland SJ, Guzman AA, Frohman EM, Monson NL. B cells from relapsing remitting multiple sclerosis patients support neuro-antigen-specific Th17 responses. J Neuroimmunol 2016;291:46–53.
6. Rounds WH, Salinas EA, Wilks TB, et al. MSPrecise: a molecular diagnostic test for multiple sclerosis using next generation sequencing. Gene 2015;572:191–197.
7. Cameron EM, Spencer S, Lazarini J, et al. Potential of a unique antibody gene signature to predict conversion to clinically definite multiple sclerosis. J Neuroimmunol 2009;213:123–130.
8. Ligocki AJ, Rivas JR, Rounds WH, et al. A distinct class of antibodies may Be an indicator of gray matter autoimmunity in early and established relapsing remitting multiple sclerosis patients. ASN Neuro 2015;7:1759091415609613.
9. Tiller T, Meffre E, Yurasov S, et al. Efficient generation of monoclonal antibodies from single human B cells by single cell RT-PCR and expression vector cloning. J Immunol Methods 2008;329:112–124.
10. Beseler C, Vollmer T, Graner M, Yu X. The complex relationship between oligoclonal bands, lymphocytes in the cerebrospinal fluid, and immunoglobulin G antibodies in multiple sclerosis: indication of serum contribution. PLoS One 2017;12:e0186842.
11. Bondt A, Hoek M, Tamara S, et al. Human plasma IgG1 repertoires are simple, unique, and dynamic. Cell Syst 2021;12:1131–1143 e5.
12. van Rijswijck DMH, Bondt A, Hoek M, et al. Discriminating cross-reactivity in polyclonal IgG1 responses against SARS-CoV-2 variants of concern. Nat Commun 2022;13:6103.
13. Bien-Ly N, Yu YJ, Bumbaca D, et al. Transferrin receptor (TfR) trafficking determines brain uptake of TfR antibody affinity variants. J Exp Med 2014;211:233–244.
14. Schindelin J, Arganda-Carreras I, Frise E, et al. Fiji: an open-source platform for biological-image analysis. Nat Methods 2012;9:676–682.
15. Katzav A, Solodeev I, Brodsky O, et al. Induction of autoimmune depression in mice by anti-ribosomal P antibodies via the limbic system. Arthritis Rheum 2007;56:938–948.
16. Galicia G, Lee DSW, Ramaglia V, et al. Isotype-switched autoantibodies are necessary to facilitate central nervous system autoimmune disease in Aicda(−/−) and Ung(−/−) mice. J Immunol 2018;201:1119–1130.
17. White MG, Emery M, Nonner D, Barrett JN. Caspase activation contributes to delayed death of heat-stressed striatal neurons. J Neurochem 2003;87:958–968.
18. Green DR. Caspases and their substrates. Cold Spring Harb Perspect Biol 2022;14:a041012.
19. McRae BL, Kennedy MK, Tan LJ, et al. Induction of active and adoptive relapsing experimental autoimmune encephalomyelitis (EAE) using an encephalitogenic epitope of proteolipid protein. J Neuroimmunol 1992;38:229–240.
20. Soellner IA, Rabe J, Mauri V, et al. Differential aspects of immune cell infiltration and neurodegeneration in acute and relapse experimental autoimmune encephalomyelitis. Clin Immunol 2013;149:519–529.
21. Wujek JR, Bjartmar C, Richer E, et al. Axon loss in the spinal cord determines permanent neurological disability in an animal model of multiple sclerosis. J Neuropathol Exp Neurol 2002;61:23–32.
22. Douglas JN, Gardner LA, Salapa HE, et al. Antibodies to the RNA-binding protein hnRNP A1 contribute to neurodegeneration in a model of central nervous system autoimmune inflammatory disease. J Neuroinflammation 2016;13:178.
23. Salapa HE, Libner CD, Levin MC. Dysfunctional RNA-binding protein biology and neurodegeneration in experimental autoimmune encephalomyelitis in female mice. J Neurosci Res 2020;98:704–717.
24. Okuda Y, Okuda M, Bernard CC. The suppression of T cell apoptosis influences the severity of disease during the chronic phase but not the recovery from the acute phase of experimental autoimmune encephalomyelitis in mice. J Neuroimmunol 2002;131:115–125.

25. Burbelo PD, Iadarola MJ, Keller JM, Warner BM. Autoantibodies targeting intracellular and extracellular proteins in autoimmunity. Front Immunol 2021;12:548469.

26. Dalmau J, Rosenfeld MR. Paraneoplastic syndromes of the CNS. Lancet Neurol 2008;7:327–340.

27. Graus F, Saiz A, Dalmau J. Antibodies and neuronal autoimmune disorders of the CNS. J Neurol 2010;257:509–517.

28. Smith KM, Budhram A, Geis C, et al. Autoimmune-associated seizure disorders. Epileptic Disord 2024;26:415–434.

29. Greenlee JE, Clawson SA, Hill KE, et al. Anti-Yo antibody uptake and interaction with its intracellular target antigen causes Purkinje cell death in rat cerebellar slice cultures: a possible mechanism for paraneoplastic cerebellar degeneration in humans with gynecological or breast cancers. PLoS One 2015;10:e0123446.

30. Greenlee JE, Clawson SA, Hill KE, et al. Purkinje cell death after uptake of anti-Yo antibodies in cerebellar slice cultures. J Neuropathol Exp Neurol 2010;69:997–1007.

31. Verschuuren J, Chuang L, Rosenblum MK, et al. Inflammatory infiltrates and complete absence of Purkinje cells in anti-Yo-associated paraneoplastic cerebellar degeneration. Acta Neuropathol 1996;91: 519–525.

32. Zhao P, Zhang N, An Z. Engineering antibody and protein therapeutics to cross the blood-brain barrier. Antib Ther 2022;5:311–331.

33. Felgenhauer K. Protein size and cerebrospinal fluid composition. Klin Wochenschr 1974;52:1158–1164.

34. Poduslo JF, Curran GL, Berg CT. Macromolecular permeability across the blood-nerve and blood-brain barriers. Proc Natl Acad Sci USA 1994;91:5705–5709.

35. Lafrance-Vanasse J, Sadekar SS, Yang Y, et al. Leveraging neonatal fc receptor (FcRn) to enhance antibody transport across the blood brain barrier. Nat Commun 2025;16:4143.

36. Trapp BD, Nave KA. Multiple sclerosis: an immune or neurodegenerative disorder? Annu Rev Neurosci 2008;31:247–269.

37. Kremenchutzky M, Rice GP, Baskerville J, et al. The natural history of multiple sclerosis: a geographically based study 9: observations on the progressive phase of the disease. Brain 2006;129:584–594.

38. Kappos L, Wolinsky JS, Giovannoni G, et al. Contribution of relapse-independent progression vs relapse-associated worsening to overall confirmed disability accumulation in typical relapsing multiple sclerosis in a pooled analysis of 2 randomized clinical trials. JAMA Neurol 2020;77:1132–1140.

39. Fisher E, Rudick RA, Simon JH, et al. Eight-year follow-up study of brain atrophy in patients with MS. Neurology 2002;59:1412–1420.

40. Klotz L, Antel J, Kuhlmann T. Inflammation in multiple sclerosis: consequences for remyelination and disease progression. Nat Rev Neurol 2023;19:305–320.

41. Hauser SL, Cree BAC. Treatment of multiple sclerosis: a review. Am J Med 2020;133:1380–1390.e2.

42. Freeman L, Longbrake EE, Coyle PK, et al. High-efficacy therapies for treatment-naïve individuals with relapsing–remitting multiple sclerosis. CNS Drugs 2022;36:1285–1299.

43. Correale J, Gaitan MI, Ysrraelit MC, Fiol MP. Progressive multiple sclerosis: from pathogenic mechanisms to treatment. Brain 2017; 140:527–546.

44. Kappos L, Butzkueven H, Wiendl H, et al. Greater sensitivity to multiple sclerosis disability worsening and progression events using a roving versus a fixed reference value in a prospective cohort study. Mult Scler 2018;24:963–973.

45. Butzkueven H, Kappos L, Pellegrini F, et al. Efficacy and safety of natalizumab in multiple sclerosis: interim observational programme results. J Neurol Neurosurg Psychiatry 2014;85:1190–1197.

46. Schmitz K, Geisslinger G, Tegeder I. Monoclonal antibodies in preclinical EAE models of multiple sclerosis: a systematic review. Int J Mol Sci 2017;18:1992.

47. Cross AH, Gelfand JM, Thebault S, et al. Emerging cerebrospinal fluid biomarkers of disease activity and progression in multiple sclerosis. JAMA Neurol 2024;81:373–383.

48. Filippi M, Preziosa P, Arnold DL, et al. Present and future of the diagnostic work-up of multiple sclerosis: the imaging perspective. J Neurol 2023;270:1286–1299.

49. Yong VW. Microglia in multiple sclerosis: protectors turn destroyers. Neuron 2022;110:3534–3548.

50. Chakravarty D, Saadi F, Kundu S, et al. CD4 deficiency causes poliomyelitis and axonal blebbing in murine coronavirus-induced neuroinflammation. J Virol 2020;94:e00548-20.

51. Dai D, Cao G, Huang S, et al. Porphyromonas gingivalis exacerbates experimental autoimmune encephalomyelitis by driving Th1 differentiation via ZAP70/NF-kappaB signaling. Front Immunol 2025;16: 1549102.

52. Khan RS, Ross AG, Willett K, et al. Amnion-derived multipotent progenitor cells suppress experimental optic neuritis and myelitis. Neurotherapeutics 2021;18:448–459.

53. Oruk S, Ergul Erkec O, Huyut Z, Acikgoz E. Neuroprotective effects of ghrelin in cuprizone-induced rat model of multiple sclerosis. Metab Brain Dis 2025;40:176.

54. Wang AA, Luessi F, Neziraj T, et al. B cell depletion with anti-CD20 promotes neuroprotection in a BAFF-dependent manner in mice and humans. Sci Transl Med 2024;16:eadi0295.